

Roles of Ligand and Oxidant in the Pd(II)-Catalyzed and Ligand-enabled C(sp³)-H Lactonization in Aliphatic Carboxylic Acid: The Mechanistic Studies

Li-Ping Xu^{*,†§}, Zhe Zhuang[†], Shaoqun Qian[†], Jin-Quan Yu^{*,‡}, Djamataddin G. Musaev^{*,†}

[†]Cherry L. Emerson Center for Scientific Computation, and Department of Chemistry, Emory University, 1521 Dickey Drive, Atlanta, GA, 30322, United States

[‡]Department of Chemistry, The Scripps Research Institute, 10550 North Torrey Pines Road, La Jolla, California 92037, United States

[§]School of Chemistry and Chemical Engineering, Shandong University of Technology, Zibo, 255000, China

ABSTRACT: The mechanism of the Pd(II)-catalyzed, mono-*N*-protected amino acid (MPAA) ligand and TBHP oxidant mediated lactonization of β -C(sp³)-H bond in aliphatic carboxylic acid has been studied. We have shown that the combination of the TBHP oxidant and MPAA ligand is very critical: the reaction proceeds via the MPAA ligand mediated Pd(II)/Pd(IV) oxidation by TBHP and following C–O reductive elimination from the Pd(IV) intermediate. While the Pd(II)/Pd(IV) oxidation is a rate-limiting step, the C–H bond activation is the regioselectivity controlling step. MPAA ligand acts as not only auxiliary ligand to stabilize the catalytic active species, but also as a proton acceptor in the C–H bond deprotonation, and as a proton donor during the Pd(II)/Pd(IV) oxidation by TBHP. The use of the peroxide-based oxidant with the hydroxyl group is absolutely necessary as well: in the rate-limiting Pd(II)/Pd(IV) oxidation transition state, H-atom of OH group participates in the 1,2-hydrogen shift to facilitate the proton-shuttling between MPAA ligand and peroxide. Thus, lactonization of the C(sp³)-H bond in aliphatic carboxylic acid occurs via the Pd(II)/Pd(IV) catalytic cycle, unlike to the previously reported Pd(II)-catalyzed, pyridone ligand and O₂ oxidant assisted benzylic C–H lactonization in aromatic *o*-methyl benzoic acid, which occurs via the Pd(II)/Pd(0) catalytic cycle and an intramolecular S_N2 nucleophilic substitution mechanism. Comparison of these findings for the C(sp³)-H bond lactonization in aliphatic and aromatic carboxylic acids enabled us to identify roles of catalyst, substrate, ligand, and oxidant.

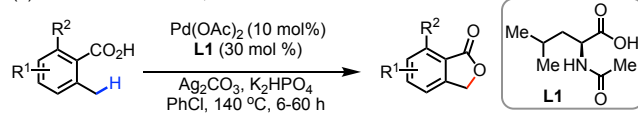
KeyWords: C–H bond lactonization, Pd(II)-catalyst, ligand controlled, MPAA ligand, aliphatic carboxylic acid, DFT calculations

INTRODUCTION

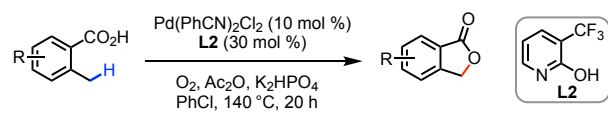
Transition metal-catalyzed selective C–H bond functionalization, i.e., conversion of “inert” C–H bonds to functional C–C and C–X (X = heteroatom) bonds, has emerged as a powerful synthetic strategy in late-stage functionalization.^{1–3} Ongoing research in this field of the chemical science has demonstrated extreme complexity of this process and has emphasized critically importance of nature of the used catalyst, substrate, solvent, base, and oxidant. Despite of numerous advances, still the search for practical, green and sustainable C–H functionalization methodologies utilizing chemically and biologically accessible substrates, and inexpensive ligands and green oxidants is continuing.⁴ It is anticipated that the discovery of the novel C–H functionalization strategies will enable syntheses of useful materials and synthons with critical C–X bonds which otherwise cannot be achieved in cost- and atom-economical ways in a large scale. In this context, catalytic C–H oxidation in the broadly accessible hydrocarbons is one of those highly active research directions, because of importance of lactones, and hydroxides in modern chemical and pharmaceutical industries.^{5–8}

Scheme 1. Pd(II)-Catalyzed C–H Lactonization with Aromatic *o*-Methyl Benzoic Acid (BA) and Aliphatic Carboxylic Acid (AA).

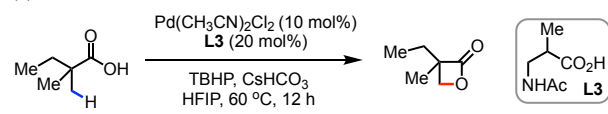
(a) Martin and coworkers, ref 10



(b) Yu and coworkers, ref 11



(c) Yu and coworkers, ref 12

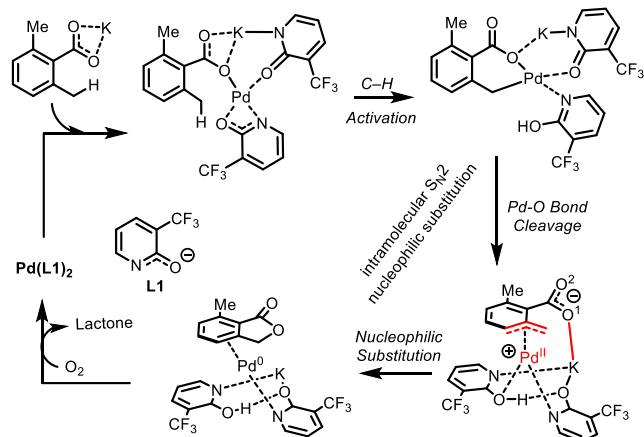


In the literature, several C–H lactonization processes were reported. For example, Chang and coworkers have developed a platinum(II)-catalyzed benzylic C–H lactonization with CuCl₂

as the oxidant.⁹ Martin and coworkers have reported a palladium-catalyzed C(sp³)-H lactonization with mono-*N*-protected β -amino acid MPAA ligand and stoichiometric silver(I) as the oxidant (**Scheme 1a**).¹⁰ Yu and coworkers have discovered a palladium(II)-catalyzed C(sp³)-H lactonization of 2,6-dimethyl benzoic acids (BA) using molecular oxygen as an oxidant (**Scheme 1b**).¹¹ In this study, the authors used pyridone as a ligand, PhCl as a solvent, and K₂HPO₄ as a base.

However, for lactonization of β -C(sp³)-H bond of aliphatic carboxylic acid (AA) by the Pd(II)-catalyst, the authors have to use MPAA as a ligand, TBHP as an oxidant, HFIP as a solvent, and CsHCO₃ as a base (**Scheme 1c**).¹² Just recently, Yu group have demonstrated that the use of a bidentate pyridine/pyridone ligand in combination with the Pd(II) pre-catalyst enables the C-H bond hydroxylation by the external oxygen molecule.¹³

Scheme 2. Previously Proposed Mechanism of the Pd(II)-Catalyzed and Pyridone Ligand Assisted C(sp³)-H Lactonization in 2,6-Dimethyl Benzoic Acid (BA).



Despite the broader application of these synthetic protocols in the late-stage functionalization,¹⁴ we anticipate that elucidation the mechanisms of the C-H bond oxidation (by internal oxidant, like C-H lactonization in carboxylic acids, or external oxidant, like C-H hydroxylation in heterocyclic carboxylic acids by O₂ molecule), as well as the roles of the utilized catalyst, substrate, ligand, base, and oxidant undoubtedly will broaden scope of these synthetic protocols and enable discovery of more efficient, environmentally benign, and highly practical novel C-H oxidation reactions. Based on these anticipations, recently, we have studied the mechanism and controlling factors of the Pd(II)-catalyzed and pyridone ligand assisted C(sp³)-H lactonization in 2,6-dimethyl benzoic acid (**Scheme 1b**, below referred as the reaction rBA).¹⁵ Briefly, we found that (see **Scheme 2**):

(a) This lactonization reaction engages the Pd(II)/Pd(0) catalytic cycle and proceeds through a stepwise *intramolecular* S_N2 nucleophilic substitution mechanism. The used molecular oxygen during the reaction oxidizes the resulted Pd(0) species and re-generates the Pd(II)-catalyst;

(b) The generated η^3 -(π -benzylic)-Pd and potassium-O(carboxylate) interactions (in red, **Scheme 2**), in course of the reaction, are critical for the success of this reaction;

(c) Consistent with the previously reported case,¹⁶ the used pyridone ligand is not only an auxiliary ligand for generation of the catalytic active species Pd(pyridone)₂, but it also serves as the deprotonating reagent in the C-H bond activation via the concerted metalation-deprotonation (CMD) transition state;

(d) The C-H bond activation is reversible, and the C-O bond formation is a rate-determining step.

Herein, we extend our previous joint computational and experimental efforts¹⁵ and are aimed to establish the mechanism of the β -C(sp³)-H bond lactonization in aliphatic carboxylic acid, previously reported by Yu and coworkers.¹² We are aiming to identify reasons why the use of MPAA ligand and TBHP oxidant (below, this reaction is referred as a rAA) was critically important for success of this reaction. We hypothesize that comparison of the obtained fundamental knowledge for this reaction with those for the previously reported¹⁵ Pd(II)-catalyzed and pyridone ligand assisted C(sp³)-H lactonization in BA will shed light on roles of ligand, oxidant, and base in the Pd(II)-catalyzed and ligand enabled C-H bond lactonization in both aromatic and aliphatic carboxylic acid substrates.

RESULTS AND DISCUSSION

I. Nature of substrate and catalytic active species under the used experimental conditions.

We initiate our discussion by identifying the true nature of substrate and active catalyst in the reported reaction conditions (see **Scheme 1c**). Calculations show that the reaction of the used aliphatic carboxylic acid with the base is exergonic (see the Supporting Information, SI), and leads to the cesium-carboxylate salt (**1**, Figure 1). Therefore, in the presented computational studies, we adopted the cesium-carboxylate (**1**) as a substrate.

Previously, we have demonstrated that in the presence of MPAA ligand, pre-catalyst Pd(II)X₂ (where X = AcO or Cl) converts to the catalytic active species of either XPd(II)(MPAA) or Pd(II)(MPAA).¹⁷⁻²² Consistently, the presented DFT calculations in this paper show that the formation of Pd(CH₃CN)₂(MPAA) (**2**, Figure 1) upon reaction of pre-catalyst Pd(CH₃CN)₂Cl₂, MPAA ligand, and CsHCO₃ base, is exergonic by 10.9 kcal/mol (here, and below, we discuss only the calculated Gibbs free energies, unless otherwise stated, while enthalpy values of the presented structures are also given in figures. See SIs for more details). Therefore, herein we adopt mononuclear Pd(CH₃CN)₂(MPAA), **2**, as the catalytic active species under the utilized experimental conditions. It should be noted that in **2**, MPAA is a di-anionic κ^2 -(*N,O*) ligand that binds to palladium with one of its carboxylic oxygens and amide nitrogen (after the deprotonation of amide N-center), which is consistent with the previous studies.¹⁷⁻²²

Having identified the nature of substrate (**1**) and active catalyst (**2**), we expect the next step of the reaction to be the substrate coordination to the Pd(II)-center of **2**. This process occurs via the exchange of two [CH₃CN] ligands by substrate **1**, and leads to the substrate-bound complex, **3**: overall reaction **(1) + (2) \rightarrow (3) + 2[CH₃CN]** is exergonic by 3.5 kcal/mol (see Figure 1). Similar to the previously reported Pd(II)-catalyzed C-H

activation in 2-benzhydrylpyridine, mediated by the [(cyclohexyloxy)carbonyl]-L-leucine ligand,¹⁷⁻²² the C¹-H¹ bond activation of AA in intermediate **3** occurs via the concerted metathesis-deprotonation (CMD) transition state **4-ts**, where the carbonyl oxygen (O¹) of the N-acetyl group of MPAA ligand acts as a proton acceptor. In transition state **4-ts**, the activated C¹-H¹ bond is 1.38 Å, and formed Pd-C¹ and H¹-O¹ bonds are 2.22 and 1.37 Å, respectively. Overcoming of 11.2 kcal/mol activation free energy barrier at transition state **4-ts** leads to formation of palladacycle **5**. Overall, the C(sp³)-H bond activation in complex **3**, i.e., reaction **3** → **4-ts** → **5** is exergonic by 6.9 kcal/mol.

The performed kinetic isotope effect (i.e. KIE) calculations for the C-H activation indicate that the C-H activation cannot a rate-controlling step: the calculated KIE 1.00.

The calculated 11.2 kcal/mol free energy barrier of the reaction **3** → **4-ts** → **5** is smaller than 18.5 kcal/mol barrier, previously reported for the C(sp³)-H bond activation of BA by the Pd(II)-coordinated pyridone ligand.¹⁵ Thus, the C(sp³)-H bond activation of AA by the MPAA ligand is more facile than the C(sp³)-H bond activation of BA by the pyridone ligand. In addition, the use of HFIP solvent may further facilitate the C(sp³)-H bond activation of AA through presumably Pd-O weak interaction or hydrogen bonding.²³ In order to better understand

roles of the ligand (MPAA vs pyridone) in the C-H bond activation in aliphatic and aromatic carboxylic acids (i.e., in the AA and BA), we have extended our study to the C-H bond activation in: (a) the aliphatic carboxylic acid with the Pd(II)-pyridone, and (b) the *o*-methyl benzoic carboxylic acid with the Pd(II)-MPAA. We find that the activation free energy barriers of these reactions are 11.2 and 15.4 kcal/mol, respectively (see SI for details). Comparison of the calculated activation barriers for these four reactions shows that the C-H bond activation in the AA and BA substrates, in general, is a facile process regardless of the nature of the used ligands (i.e., MPAA or pyridone).

II. C-O bond formation

II.1 Direct C-O reductive elimination. From the generated palladacycle **5**, the lactonization process is expected to proceed via the C¹-O² bond formation. As previously we have discussed,¹⁵ the C-O bond formation from the Pd(II) and/or high-valent Pt and Pd-complexes is a complicated process.²⁴⁻³³ Success of this process is not only dependent on the nature and oxidation state of the used transition metals, but also on the nature of the auxiliary ligands, oxidant, and base. For example, multiple experimental groups²⁷⁻³² have provided evidences that C-O bond formation in the Pd(IV) and Pt(IV)-complexes may proceed via either direct reductive elimination or/and stepwise S_N2 nucleophilic substitution mechanisms.

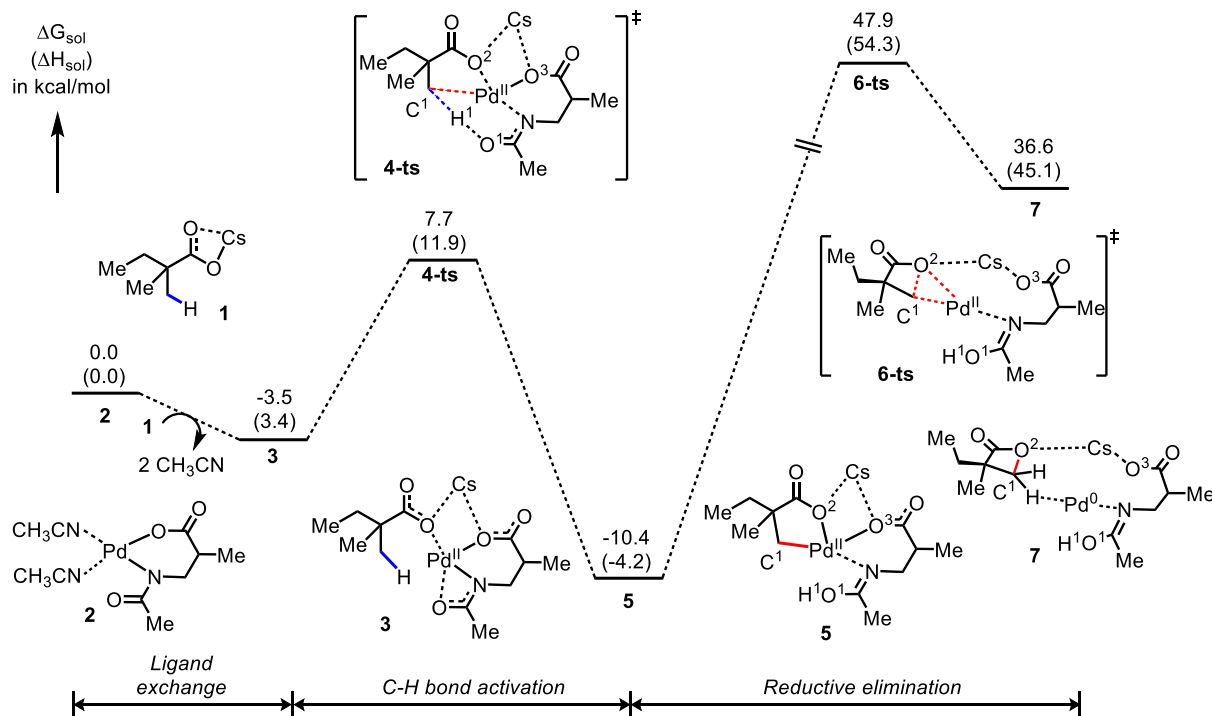


Figure 1. Energy profile for the ligand exchange, C-H bond activation, and direct C-O reductive elimination steps for the β -C(sp³)-H lactonization with aliphatic carboxylic acid catalyzed by the MPAA-ligated Pd(II) complex.

However, in the literature, only rare mechanistic studies on the C-O bond formation from the Pd(II)-complexes were reported. In 2011, Hartwig and coworkers have reported the C(sp³)-O reductive elimination from the *bis*-phosphine-ligated

Pd(II)-aryloxide complexes, and have established an ionic mechanism including the dissociation of ArO⁻, followed by nucleophilic attack of ArO⁻ anion on the cationic benzyl-palladium species.³³ In 2011, Martin and coworkers have proposed

a concerted reductive elimination mechanism for the Pd(II)-catalyzed $C(sp^3)$ -H lactonization with stoichiometric silver(I) oxidant,¹⁰ however, they have not ruled out a stepwise mechanism including the dissociation of the carboxylate ligand and following C–O bond formation. Just recently, our group have proposed and validated a stepwise *intramolecular* S_N2 nucleophilic substitution mechanism of the Pd(II)-catalyzed and pyridone ligand-enabled lactonization in *o*-methyl benzoic acid, which utilizes K_2HPO_4 as a base, and O_2 as an oxidant.¹⁵

Armed with this knowledge, here, we start our analysis of the C–O bond formation in intermediate **5** by the direct reductive elimination mechanism. We found that the associated C–O reductive elimination free energy barrier (58.3 kcal/mol, at the associated transition state **6-ts**, Figure 1) for this process is prohibitively high, indicating that the direct $C(sp^3)$ -O reductive elimination is unlikely in aliphatic carboxylic acid complex by the Pd(II) catalyst $Pd(CH_3CN)_2(MPAA)$, **2**.

II.2 Stepwise C–O formation. Next, we studied the stepwise $C(sp^3)$ -O bond formation in palladacycle **5**. As previously shown for the C–O bond formation in palladacycle with the aromatic carboxylic acid, i.e. reaction rBA, it proceeds through the stepwise pathway that occurs via the Pd–O²(O=)CR bond dissociation and the following intramolecular S_N2 nucleophilic substitution steps (see **Scheme 2**). All our attempts to locate transition state associated with the Pd–O²(O=)CR bond cleavage in intermediate **5** have led to structure **8-ts** (Figure 2), where the simultaneous Pd–O² and C¹–H^α bond cleavage, and complementing C¹–O² and Pd–H^α bond formation occur. This step occurs by 44.5 kcal/mol energy barrier and leads to intermediate **9**, which is 33.0 kcal/mol higher in free energy than pre-reaction complex **5**. Close analyses of **9** show that in this structure the formation of the Pd–C¹, Pd–H^α, and C¹–O² bonds, and the cleavage of the Pd–O² and C¹–H^α bonds are completed. The following C¹–H^α reductive elimination in **9** to form the Pd(II)-coordinated lactone, **11**, is the rate-determining step of the investigated stepwise pathway that requires an overall of 51.9 kcal/mol free energy barrier (at **10-ts** relative to **5**). Above presented energetics (Figure 2) show that, the stepwise C–O bond formation in the C–H activation product **5**, which was the most favorable mechanism of the reaction with aromatic benzoic acid (i.e. reaction rBA), is not practical for the Pd(II)-catalyzed and MPAA ligand-enabled lactonization of β -C(sp^3)-H bond in aliphatic carboxylic acid (i.e. reaction rAA). Our analyses show that the transition state **10-ts** lacks the stabilizing η^3 -(π -benzylic)–Pd(II) interaction. This could be (as emphasized previously¹⁵) one of the reasons for the calculated large C–O bond formation barrier. Thus, the reaction rAA, most likely, proceeds via the different mechanistic pathway than the intramolecular S_N2 nucleophilic substitution pathway previously reported for the reaction rBA.¹⁵

II.3 TBHP oxidative addition and the Pd(II)/Pd(IV) oxidation. Thus, above presented computational data showed that neither direct reductive elimination nor the stepwise intramolecular S_N2 nucleophilic substitution mechanisms for the C(sp^3)-O bond formation in palladacycle **5** are the productive pathways of the Pd(II)-catalyzed and MPAA ligand-enabled β -C(sp^3)-H lactonization in aliphatic carboxylic acid. However, the above

presented studies are based on the assumption that the oxidant *does not facilitate the C(sp^3)-O bond formation*: this assumption was based on our previous findings for the Pd(II)-catalyzed and pyridone ligand-enabled C(sp^3)-H lactonization in aromatic carboxylic acid, which utilized O_2 as an oxidant.¹⁵ Below, we re-visit this assumption and re-investigate role of oxidant TBHP in the C(sp^3)-O bond formation during the reaction rAA. Previous studies of the Pd(II)-catalyzed Wacker oxidation of alkenes, as well as the Sharpless-Katsuki epoxidation by the dinuclear titanium complex with TBHP as the oxidant have shown that TBHP might act as the oxygen source.^{34,35,36} However, to the best of our knowledge, in literature there is no precedent of oxidative addition of TBHP to the Pd(II) species.

The presented calculations show that addition of TBHP to palladacycle **5** results in the formation of the **5-TBHP** adduct: the energetically most favorable isomers of this adduct are complexes **12** and **14** with stabilization free energy of 6.6 and 3.5 kcal/mol, respectively (Figure 3). As seen from Figure 3, in adduct **12**, TBHP is coordinated to Pd-center via its O^tBu end. As a result, it displaces the Cs–O³(ligand) interaction and forms the Pd–O^tBu and Cs–OH–O(ligand) bonds. In the energetically less favorable adduct **14**, TBHP is coordinated to Pd-center with its hydroxyl oxygen (O⁴) without displacement of the Cs–O³(ligand) interaction.

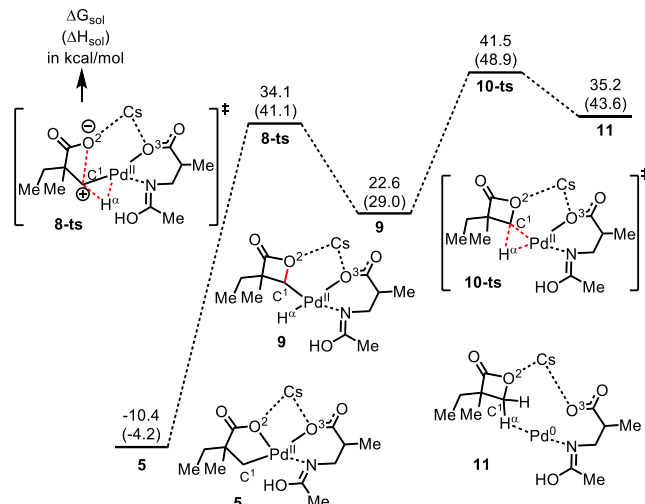


Figure 2. The stepwise $C(sp^3)$ -O bond formation in palladacycle **5** with aliphatic carboxylic acid.

The calculations also show that the classical oxidative addition of TBHP to Pd(II), that proceeds via a three-centered transition state **13-ts**, requires prohibitively (by 42.6 kcal/mol) high free energy barrier. This finding is consistent with lack of precedent of oxidative addition of TBHP to Pd(II) species in the literature. Here we will not discuss this process in detail, while we include all associated structures of this direct oxidative addition pathway in the Supporting Information.

Gratifyingly, we find the kinetically most favorable pathway for the Pd(II)/Pd(IV) oxidation by TBHP, initiated directly from the energetically less favorable conformer **14** (below, we will consider **14** and **12** structures as a Curtin-Hammett equilibrium, and will report the calculated energies from the most favorable isomer **12**).

As seen in Figure 3, in complex **14**, TBHP is coordinated to the Pd center from the same side as the N-center of the MPAA ligand. This structural motif (previously reported²⁰ as a *cis* coordination motif) makes possible involvement of the monoanionic imine ligand and in the TBHP O–O bond activation and Pd(II)/Pd(IV) oxidation. Indeed, in the associated transition state **15-ts** (see also Figure 4), not only the *t*BuO–OH bond is breaking and the Pd–O⁴(H) bond is forming, but also the 1,2-hydrogen shift (i.e. H²) within the TBHP takes place: from its Pd-coordinated O⁴–center to the O*t*Bu fragment. Simultaneously with these bond-breaking and bond-formation events within the TBHP-fragment, the hydrogen atom (i.e. H¹) of hydroxyl group of the previously protonated MPAA ligand (i.e. imine ligand) is transferring to the Pd-coordinated O⁴ atom of TBHP. This transformation results in generation of the Pd-coordinated amide center.

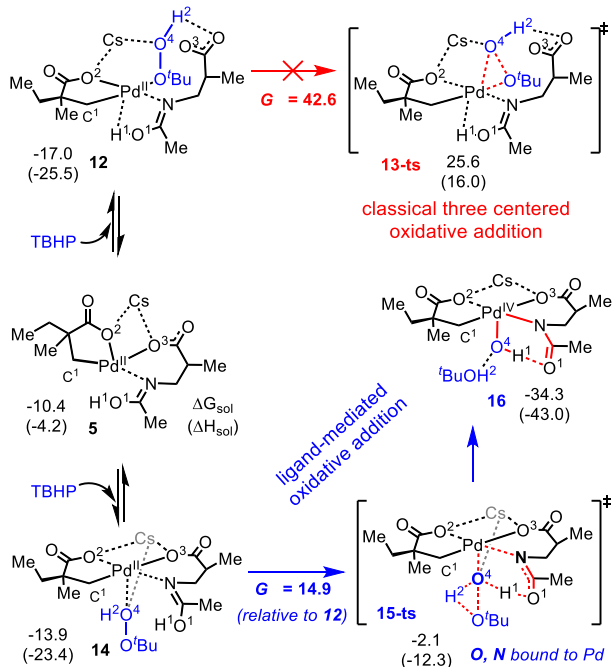


Figure 3. The studied classical and ligand-mediated oxidative addition of TBHP to intermediate **5**.

As a result of these multi-component complex transformations, (a) Pd(II) is oxidized to Pd(IV), (b) the oxygen atom (O⁴) from the hydroxyl group of TBHP and the nitrogen atom of MPAA become the two X-type ligand atoms (i.e. the reduced centers) that bind to the metal center, (c) MPAA ligand transforms from the mono-anionic bidentate-coordinated ligand in **14** to the di-anionic bidentate-coordinated one in the oxidative addition product **16**, and (d) the *t*BuO group of TBHP transforms to *t*BuOH. Here, we labeled this complex transformation as a *MPAA ligand mediated Pd(II)/Pd(IV) oxidation by TBHP*. This process has an overall of 14.9 kcal/mol free energy barrier relative to the energetically most favorable pre-reaction complex **12**. Furthermore, the overall reaction **12** → **15-ts** → **16** is exergonic by 17.3 kcal/mol. *Thus, the use of the MPAA ligand in combination with TBHP oxidant is critical for promoting of the Pd(II)/Pd(IV) oxidation in course of the β -C(sp³)–H bond lactonization in aliphatic carboxylic acid (AA).*

Here, we should mention that our calculations (see the Supporting Information) shown that the pyridone ligand enabled Pd(II)/Pd(IV) oxidation with TBHP oxidant requires 22.0

kcal/mol free energy barrier. Comparison of this value with the 14.9 kcal/mol energy barrier for the MPAA ligand mediated Pd(II)/Pd(IV) oxidation by TBHP indicates that the use of MPAA ligand could be better than pyridone ligand in the β -C(sp³)–H bond lactonization of aliphatic carboxylic acid (AA) by the Pd-catalyst and TBHP oxidant.

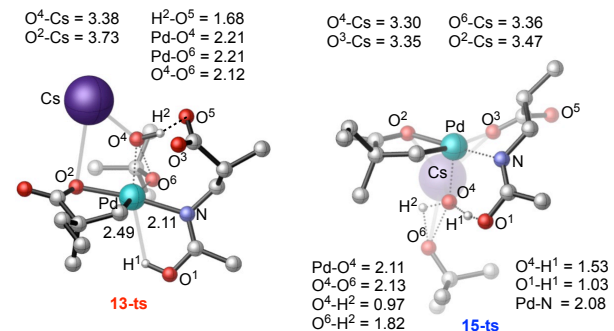


Figure 4. Geometries of the classical (**13-ts**) and ligand-mediated (**15-ts**) oxidative addition transition states (some hydrogen atoms are omitted for clarity, and bond distances are given in Å).

II.4 Reductive elimination and catalyst regeneration. As it could be anticipated, after the *MPAA ligand mediated Pd(II)/Pd(IV) oxidation by TBHP*, the C(sp³)–O (i.e. C¹–O², see Figure 5) reductive elimination from the Pd(IV)-intermediate takes place with a small (by 11.1 kcal/mol) free energy barrier at the transition state **17-ts** that leads to the complex **18** with the Pd-coordinated lactone (Figure 5). This step is exergonic by 17.5 kcal/mol. Finally, the addition of the second equivalent of substrate, and dissociation of lactone and *t*BuOH regenerates the pre-reaction intermediate (**3**), which would enter the next catalytic cycle. Final step of the reaction (Figure 5) is endergonic by 16.7 kcal/mol but is feasible under the reported experimental conditions.

Above presented “*MPAA ligand mediated Pd(II)/Pd(IV) oxidation by TBHP*” phenomena demonstrates the critical importance of not only the use of the MPAA ligand, but also the presence of the hydroxyl group in the peroxide-based oxidants. Indeed, in the rate-limiting Pd(II)/Pd(IV) oxidation transition state **15-ts**, H-atom of the TBHP oxidant participates in the 1,2-hydrogen shift that facilitates the proton-shuttling between imine ligand and the Pd-coordinated hydroxyl oxygen of the peroxide. This finding enables us to conclude that the peroxide-based oxidants with no hydroxyl group, such as *t*BuOO*t*Bu, BzOOBz, BzOO*t*Bu, Lauroyl peroxide etc., are going to be poor Pd(II)/Pd(IV) oxidants in the Pd(II)-catalyzed and MPAA ligand-enabled lactonization of β -C(sp³)–H bond in aliphatic carboxylic acid. This conclusion is consistent with the available experiments showing no or little³⁷ lactonization with peroxide-based oxidants with no hydroxyl group.¹²

Thus, above presented findings show that overall, the Pd(II)-catalyzed and MPAA ligand-enabled β -C(sp³)–H lactonization in aliphatic carboxylic acid proceeds via the Pd(II)/Pd(IV) catalytic cycle that includes: (a) the MPAA ligand assisted C–H bond activation via the CMD mechanism and the followed oxidant coordination to the C–H bond activation product; (b) the MPAA ligand mediated Pd(II)/Pd(IV) oxidation by TBHP; (c) the

$C(sp^3)$ -O reductive elimination from the Pd(IV) intermediate; and (d) catalytic active species regeneration. While the MPAA ligand mediated Pd(II)/Pd(IV) oxidation by TBHP is the rate-determining step of the reaction, the regioselectivity controlling step of the reaction is the C-H bond activation because the reverse C-H bond formation barrier is larger (24.7 kcal/mol) than the forward Pd(II)/Pd(IV) oxidation by TBHP (14.9 kcal/mol, relative to intermediate **12**).

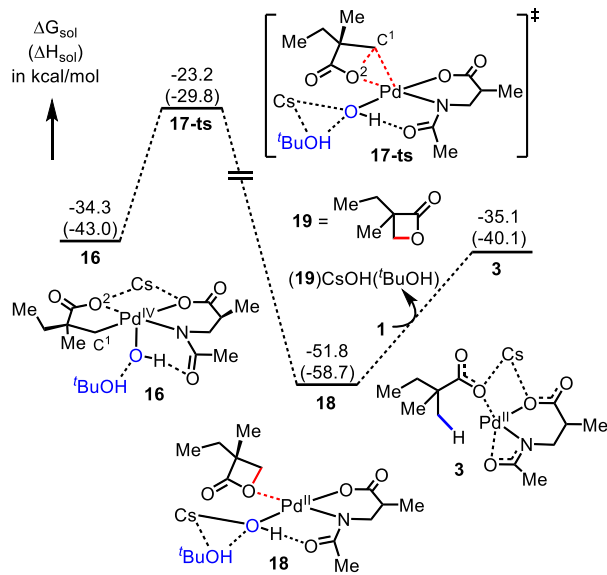


Figure 5. Energy profile for the C-O reductive elimination in Pd(IV)-intermediate **16**, and the catalyst regeneration from intermediate **18**.

III. Selective β -primary, β -secondary, and γ -primary C-H bond lactonization in aliphatic carboxylic acid.

To validate above made conclusion on the regioselectivity controlling C-H activation step of the reaction, we have calculated the β -primary, β -secondary, and γ -primary C-H bond activation barriers in the utilized aliphatic carboxylic acid (**1**). These calculations (see Figure 6), consistent with available experiments,¹² show that the β -primary C-H bond activation requires less energy barrier (11.2 kcal/mol, at the transition state **4-ts**), than the β -secondary (14.1 kcal/mol, at the transition state **4s-ts**), and γ -primary (13.6 kcal/mol, at the transition state **4r-ts**) C-H bond activations (see Figure 6a and 6b).

To gain insights into the regioselectivity-controlling factors, we performed the distortion/interaction analyses.³⁸⁻⁴⁵ In these analyses, the (aliphatic carboxylic)-cesium unit is assigned to be the substrate (*sub*), and the remaining part of the system is labeled as a catalyst (*cat*) (see SIs for more details). Data presented in Figure 6a show that the calculated difference between the β -primary (**4-ts**) and β -secondary (**4s-ts**) C-H bond activation barriers is, mostly, due to the larger unfavorable distortion of substrate in transition state **4s-ts** (Figure 6a). This is well reflected by the corresponding geometries.⁴⁶ However, the calculated difference between the β -primary (**4-ts**) and γ -primary (**4r-ts**) C-H bond activation barriers is result of both the larger unfavorable distortion and smaller *sub-cat* interaction energies in **4r-ts**.

The calculated larger distortion energy in **4r-ts** compared to **4-ts** can be explained by the formation of the six-membered vs five-membered ring chelated palladacycle, respectively.^{47,48} The smaller *sub-cat* interaction energy in **4r-ts** compared to **4-ts** is manifested in (a) the calculated Pd-O bond distances, and (b) the donor-acceptor interaction energy ($E^{(2)ij}$) between the lone-pair of oxygen n(O) of *sub* with unoccupied d_{2z}^* orbital of Pd(II)-center in these transition states, respectively (Figure 6c).

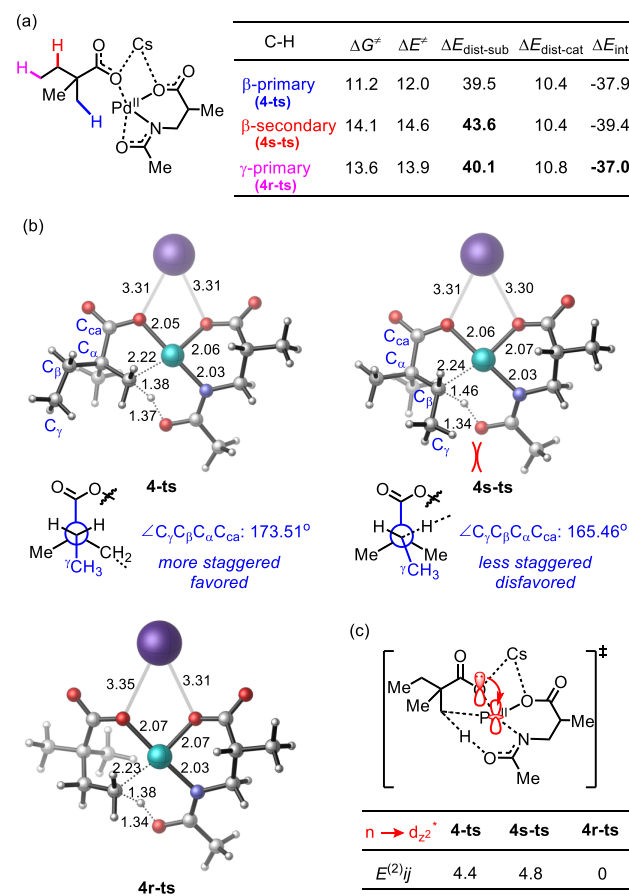


Figure 6. (a) Calculated free energy barriers for different C-H bond activations, and results of the distortion/interaction analysis; (b) Geometry structures for the studied C-H bond activation transition states; (c) NBO second-order perturbative interaction analysis (energies and bond distances are given in kcal/mol and Å, respectively).

CONCLUSIONS

Comparison of key mechanistic details of the Pd(II)-catalyzed and pyridone ligand assisted $C(sp^3)$ -H lactonization in aromatic *o*-methyl benzoic acid (BA) (reaction rBA),¹⁵ and the Pd(II)-catalyzed and MPAA ligand-enabled lactonization of β -C(sp^3)-H lactonization in aliphatic carboxylic acid (AA) (reaction rAA) has shown that (see Scheme 3):

- True substrates and catalytic active species of both reactions are the counter-cation (from the base) coordinated original organic substrate, and the Pd(II)-ligand (pyridone or MPAA) system, respectively.

(b) In both reactions, the targeted C–H bond cleavage occurs via the concerted metalation-deprotonation (CMD) mechanism, where the Pd(II)-coordinated anionic ligand (pyridone or MPAA, respectively) acts as a proton acceptor.

(c) In the reaction rBA, the C–O bond formation proceeds via the *intramolecular S_N2* nucleophilic substitution mechanism via the rate-determining transition state with the η^3 -(π -benzylic)–Pd(II) interaction.¹⁵ The presence of the η^3 -(π -benzylic)–Pd(II) and the potassium–O(carboxylate) interactions are critical for the C–O formation.

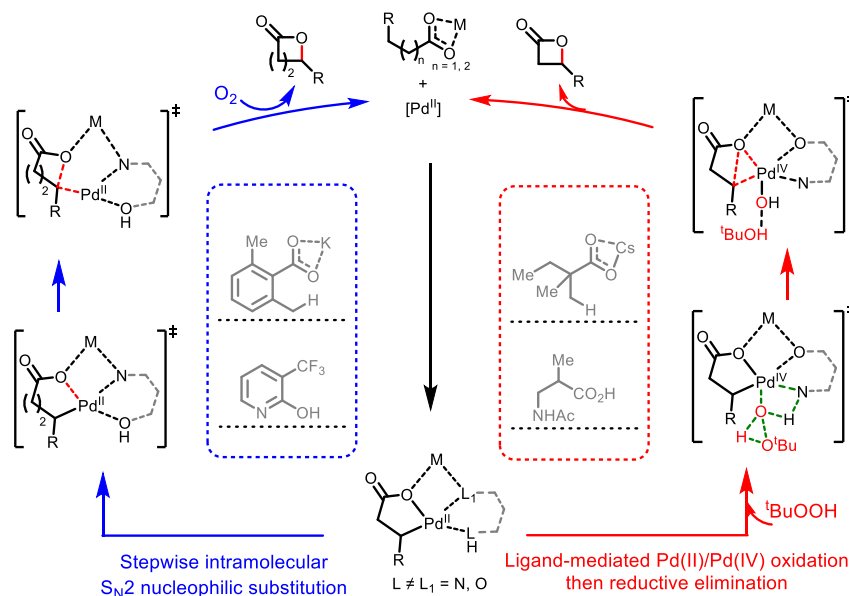
(d) Lack of the stabilizing η^3 -(π -benzylic)–Pd(II) interaction, in course of the reaction rAA, makes the *intramolecular S_N2* nucleophilic substitution mechanism of the β -C(sp³)–H lactonization in aliphatic carboxylic acid by the Pd(II)/MPAA catalyst not feasible. Astoundingly, the use of TBHP oxidant, in combination with the MPAA ligand, opened energetically more favorable reaction path, which we called as *MPAA ligand mediated Pd(II)/Pd(IV) oxidation by TBHP then the C–O reductive elimination from the Pd(IV) intermediate pathway*. Overall, this unprecedented mechanistic pathway requires 14.9 kcal/mol free energy barrier (for the Pd(II)/Pd(IV) oxidation) and is exergonic by 17.3 kcal/mol.

(e) The use of MPAA ligand in the reaction rAA is critically important: it acts as a proton acceptor in the C–H bond deprotonation, and as a proton donor during the Pd(II)/Pd(IV) oxidation by TBHP.

(f) Equally, the use of the peroxide-based oxidants, such as RO-OH, with the hydroxyl group is necessary because, in the rate-limiting Pd(II)/Pd(IV) oxidation transition state, H-atom of this group participates in the 1,2-hydrogen shift that facilitates the proton-shuttling between imine ligand (of MPAA) and coordinated peroxide oxygen. To the best of our knowledge, it is the first demonstration of the *Pd(II)/Pd(IV) oxidation by TBHP*. However, one also should comment that peroxides like mCPBA and CMHP with the hydroxyl group, but highly complex R-fragments may require special attentions.

Thus, above presented data show that outcome of the Pd(II)-catalyzed and ligand enabled C–H bond lactonization is critically dependent on the nature of substrate, oxidant, ligand, and base. We believe that uncovered intimate insights in this work will enable our colleagues in designing more efficient Pd(II)-catalyzed C–H bond lactonization strategies applicable for the wide scope of substrate.

Scheme 3. The Mechanisms of the Pd(II)-Catalyzed and Pyridone Ligand Assisted Lactonization of C(sp³)–H in Aromatic o-Methyl Benzoic Acid (left), and the Pd(II)-Catalyzed and MPAA Ligand-Enabled Lactonization of β -C(sp³)–H in Aliphatic Carboxylate Acid (right).



Computational Details

All the geometry optimizations were performed using Gaussian 09 suit of program⁴⁹ at the B3LYP⁵⁰⁻⁵² density functional powered by Grimme's empirical dispersion-correction (D3)⁵³ (denoted as B3LYP-D3). Lanl2dz/6-31G(d,p) basis sets were used for Pd, Cs/all-other-atoms respectively, in which the Hay-Wadt effective core potentials^{54,55} were considered for Pd and Cs. Single point energy calculations were performed at the

optimized geometries using the SDD/6-311++G(d,p) basis sets for Pd,Cs/all-other-atoms. Frequency calculations at the same level of theory as the geometry optimizations confirmed the nature of the reported stationary structures and provided thermal corrections to the energies. Intrinsic reaction coordinate (IRC) calculations were performed for selected transition states to ensure their true nature and properly connect reac-

tants and products. Solvent effects were incorporated in geometry optimizations, frequency calculations, and single point energy calculations at the SMD⁵⁶ solvent model. 2-methyl-1-propanol is used to mimic of the HFIP as it has the closest dielectric parameters with HFIP. 3D geometries were prepared using CYLView software.⁵⁷ $\Delta G_{\text{sol}}(\Delta H_{\text{sol}})$ (in kcal/mol) are given in figures unless otherwise stated.

SUPPORTING INFORMATION: Reaction energies of the cesium carboxylate (**1**) and active catalyst (**2**) formation; The C–H bond activation in aliphatic carboxylic acid catalyzed by the Pd(II)-catalyst and pyridone ligand; The bond activation in *o*-methyl benzoic acid catalyzed by the Pd(II)-catalyst and MPAA ligand; The calculated C–H bond activation barriers in aliphatic carboxylic acid with the Pd(II)-pyridone, and *o*-methyl benzoic carboxylic acid with the Pd(II)-MPAA; The classical Pd(II)/Pd(IV) oxidation by TBHP; The details of the distortion/interaction analyses; The details of the pyridone ligand mediated Pd(II)-to-Pd(IV) oxidation by TBHP oxidation; The classical Pd(II)/Pd(IV) oxidation by AcOO^tBu; Full free energy profile of the reaction; C–O reductive elimination from the Pd(II) intermediate with one additional CH₂ moiety in substrate; Energies and cartesian coordinates for all calculated species; Additional References.

ASSOCIATED CONTENT

Supporting Information. Energetics and Cartesian coordinates for all reported structures. This material is available free of charge via the Internet at <http://pubs.acs.org>.

AUTHOR INFORMATION

Corresponding Author

[*zulp@sdut.edu.cn](mailto:zulp@sdut.edu.cn)

[*dmusaev@emory.edu](mailto:dmusaev@emory.edu)

[*yu200@scripps.edu](mailto:yu200@scripps.edu)

Notes

The authors declare no competing financial interest.

ACKNOWLEDGMENT

This work was supported by the National Science Foundation under the CCI Center for Selective C–H Functionalization (CHE-1700982). The authors gratefully acknowledge the use of the resources of the Cherry Emerson Center for Scientific Computation at Emory University. L.-P. Xu acknowledges the Natural Science Foundation of China (NSFC 21702126) and the China Scholarship Council for support.

REFERENCES

1. Chen, X.; Engle, K. M.; Wang, D.-H.; Yu, J.-Q., Palladium(II)-Catalyzed C–H Activation/C–C Cross-Coupling Reactions: Versatility and Practicality. *Angew. Chem. Int. Ed.* **2009**, *48*, 5094–5115.
2. Lyons, T. W.; Sanford, M. S., Palladium-Catalyzed Ligand-Directed C–H Functionalization Reactions. *Chem. Rev.* **2010**, *110*, 1147–1169.
3. He, J.; Wasa, M.; Chan, K. S. L.; Shao, Q.; Yu, J.-Q., Palladium-Catalyzed Transformations of Alkyl C–H Bonds. *Chem. Rev.* **2017**, *117*, 8754–8786.
4. Hu, M.; Wu, W.; Jiang, H., Palladium-Catalyzed Oxidation Reactions of Alkenes with Green Oxidants. *ChemSusChem*. **2019**, *12*, 2911–2935.
5. Kang, E. J.; Lee, E., Total Synthesis of Oxacyclic Macrodiolide Natural Products. *Chem. Rev.* **2005**, *105*, 4348–4378;
6. Faul, M. M.; Huff, B. E., Strategy and Methodology Development for the Total Synthesis of Polyether Ionophore Antibiotics. *Chem. Rev.* **2000**, *100*, 2407–2474.
7. Zhao, J.; Feng, J.; Tan, Z.; Liu, J.; Zhao, J.; Chen, R.; Xie, K.; Zhang, D.; Li, Y.; Yu, L.; Chen, X.; Dai, J., Stachybotrysins A–G, Phenylspirodromane Derivatives from the Fungus Stachybotrys chartarum. *J. Nat. Prod.* **2017**, *80*, 1819–1826;
8. Masiulis, S.; Desai, R.; Uchański, T.; Serna Martin, I.; Laverty, D.; Karia, D.; Malinauskas, T.; Zivanov, J.; Pardon, E.; Kotecha, A.; Steyaert, J.; Miller, K. W.; Aricescu, A. R., GABAA Receptor Signalling Mechanisms Revealed by Structural Pharmacology. *Nature* **2019**, *565*, 454–459.
9. Lee, J. M.; Chang, S., Pt-Catalyzed sp³ C–H Bond Activation of o-alkyl Substituted Aromatic Carboxylic Acid Derivatives for the Formation of Aryl Lactones. *Tetrahedron Lett.* **2006**, *47*, 1375–1379.
10. Novák, P.; Correa, A.; Gallardo-Donaire, J.; Martin, R., Synergistic Palladium-Catalyzed C(sp³)–H Activation/C(sp³)–O Bond Formation: A Direct, Step-Economical Route to Benzolactones. *Angew. Chem. Int. Ed.* **2011**, *50*, 12236–12239.
11. Qian, S.; Li, Z.-Q.; Li, M.; Wisniewski, S. R.; Qiao, J. X.; Richter, J. M.; Ewing, W. R.; Eastgate, M. D.; Chen, J. S.; Yu, J.-Q., Ligand-Enabled Pd(II)-Catalyzed C(sp³)–H Lactonization Using Molecular Oxygen as Oxidant. *Org. Lett.* **2020**, *22*, 3960–3963.
12. Zhuang, Z.; Yu, J.-Q., Lactonization as A General Route to β-C(sp³)–H Functionalization. *Nature* **2020**, *577*, 656–659.
13. Li, Z.; Wang, Z.; Chekshin, N.; Qian, S.; Qiao, J. X.; Cheng, P. T.; Yeung, K.-S.; Ewing, W. R.; Yu, J.-Q., A Tautomeric Ligand Enables Directed C–H Hydroxylation with Molecular Oxygen. *Science*, **2021**, *372*, 1452–1457.
14. Moir, M.; Danon, J. J.; Reekie, T. A.; Kassiou, M., An Overview of Late-stage Functionalization in Today's Drug Discovery. *Expert Opin. Drug Discov.* **2019**, *14*, 1137–1149.
15. Xu, L.-P.; Qian, S.; Zhuang, Z.; Yu, J.-Q.; Musaev, D. G., Unconventional Mechanism and Selectivity of the Pd(II)-Catalyzed C(sp³)–H vs C(sp²)–H Bond Lactonization in Aromatic Carboxylic Acid. *Nat. Commun.* **2022**, *13*, 1–8.
16. Wang, P.; Verma, P.; Xia, G.; Shi, J.; Qiao, J. X.; Tao, S.; Cheng, P. T. W.; Poss, M. A.; Farmer, M. E.; Yeung, K.-S.; Yu, J.-Q., Ligand-accelerated Non-directed C–H Functionalization of Arenes. *Nature* **2017**, *551*, 489–493.
17. Musaev, D. G.; Kaledin, A.; Shi, B.-F.; Yu, J.-Q., Key Mechanistic Features of Enantioselective C–H Bond Activation Reactions Catalyzed by [(Chiral Mono-N-Protected Amino Acid)-Pd(II)] Complexes. *J. Am. Chem. Soc.* **2012**, *134*, 1690–1698.
18. Musaev, D. G.; Figg, T. M.; Kaledin, A. L., Versatile Reactivity of Pd-catalysts: Mechanistic Features of the Mono-N-Protected Amino Acid Ligand and Cesium-halide Base in Pd-catalyzed C–H Bond Functionalization. *Chem. Soc. Rev.* **2014**, *43*, 5009–5031.
19. Cheng, G.-J.; Yang, Y.-F.; Liu, P.; Chen, P.; Sun, T.-Y.; Li, G.; Zhang, X.; Houk, K. N.; Yu, J.-Q.; Wu, Y.-D., Role of N-Acyl Amino Acid Ligands in Pd(II)-Catalyzed Remote C–H Activation of Tethered Arenes. *J. Am. Chem. Soc.* **2014**, *136*, 894–897.
20. Haines, B. E.; Musaev, D. G., Factors Impacting the Mechanism of the Mono-N-Protected Amino Acid Ligand-Assisted and Directing-Group-Mediated C–H Activation Catalyzed by Pd(II) Complex. *ACS Catal.* **2015**, *5*, 830–840.
21. Cheng, G.-J.; Chen, P.; Sun, T.-Y.; Zhang, X.; Yu, J.-Q.; Wu, Y.-D., A Combined IM – MS/DFT Study on [Pd(MPAA)]-Catalyzed Enantioselective C–H Activation: Relay of Chirality through a Rigid Framework. *Chem. Eur. J.* **2015**, *21*, 11180–11188.
22. Gair, J. J.; Haines, B. E.; Filatov, A. S.; Musaev, D. G.; Lewis, J. C. Mono- N -Protected Amino Acid Ligands Stabilize Dimeric Palladium(II) Complexes of Importance to C–H Functionalization. *Chem. Sci.* **2017**, *8*, 5746–5757.
23. Bhattacharya, T.; Ghosh, A.; Maiti, D., Hexafluoroisopropanol: The Magical Solvent for Pd-catalyzed C–H Activation. *Chem. Sci.* **2021**, *12*, 3857–3870.

24. Williams, B. S.; Goldberg, K. I., Studies of Reductive Elimination Reactions To Form Carbon–Oxygen Bonds from Pt(IV) Complexes. *J. Am. Chem. Soc.* **2001**, *123*, 2576-2587.

25. Ananikov, V.P.; Musaev, D. G.; Morokuma, K., Critical Effects of Phosphine Ligands on the Mechanism of Carbon–Carbon Bond Formation Involving Palladium(II) Complexes. A Theoretical Evaluation of Steric and Electronic Factors. *Eur. J. Inorg. Chem.* **2007**, *34*, 5390-5399.

26. Ananikov, V. P.; Musaev, D. G.; Morokuma, K., Vinyl–Vinyl Coupling on Late Transition Metals through C–C Reductive Elimination Mechanism. A Computational Study. *J. Am. Chem. Soc.* **2002**, *124*, 2839-2852.

27. Dick, A. R.; Kampf, J. W.; Sanford, M. S., Unusually Stable Palladium(IV) Complexes: Detailed Mechanistic Investigation of C–O Bond-Forming Reductive Elimination. *J. Am. Chem. Soc.* **2005**, *127*, 12790-12791.

28. Liu, G.; Stahl, S. S., Highly Regioselective Pd-Catalyzed Intermolecular Aminoacetoxylation of Alkenes and Evidence for *cis*-Aminopalladation and S_N2 C–O Bond Formation. *J. Am. Chem. Soc.* **2006**, *128*, 7179-7181.

29. Camasso, N. M.; Perez-Temprano, M. H.; Sanford, M. S., C(sp³)-O Bond-Forming Reductive Elimination from Pd(IV) with Diverse Oxygen Nucleophiles. *J. Am. Chem. Soc.* **2014**, *136*, 12771-12775.

30. Carty, A. J.; AriaFard, A.; Camasso, N. M.; Higgs, A. T.; Yates, B. F.; Sanford, M. S., Computational Study of C(sp³)-O Bond Formation at A Pd(IV) Centre. *Dalton Trans.* **2017**, *46*, 3742-3748.

31. Park, H.; Verma, P.; Hong, K.; Yu, J. Q., Controlling Pd(IV) Reductive Elimination Pathways Enables Pd(II)-catalysed Enantioselective C(sp³)-H Fluorination. *Nat. Chem.* **2018**, *10*, 755-762.

32. Powers, D. C.; Geibel, M. A. L.; Klein, J. E. M. N.; Ritter, T., Bimetallic Palladium Catalysis: Direct Observation of Pd(III)-Pd(III) Intermediates. *J. Am. Chem. Soc.* **2009**, *131*, 17050-17051.

33. Marquard, S. L.; Hartwig, J. F., C(sp³)-O Bond-Forming Reductive Elimination of Ethers from Bisphosphine-Ligated Benzylpalladium(II) Aryloxide Complexes. *Angew. Chem. Int. Ed.* **2011**, *50*, 7119-7123.

34. Cornell, C. N.; Sigman, M. S., Discovery of and Mechanistic Insight into a Ligand-Modulated Palladium-Catalyzed Wacker Oxidation of Styrenes Using TBHP. *J. Am. Chem. Soc.* **2005**, *127*, 2796-2797.

35. Michel, B. W.; Steffens, L. D.; Sigman, M. S., On the Mechanism of the Palladium-Catalyzed tert-Butylhydroperoxide-Mediated Wacker-Type Oxidation of Alkenes Using Quinoline-2-Oxazoline Ligands. *J. Am. Chem. Soc.* **2011**, *133*, 8317-8325.

36. Katsuki, T.; Sharpless, B. K. "The first practical method for asymmetric epoxidation". *J. Am. Chem. Soc.* **1980**, *102*, 5974-5976.

37. It should be noted that AcOO^tBu that bears no hydroxyl group also promotes of this reaction but with much less yield (34%) compared to that of TBHP (73 %). Since our calculations of the classical oxidative addition of AcOO^tBu to Pd(II) shown (see Figure S7 in the Supporting Informations) a dramatically high (ca 40.3 kcal/mol) activation free energy barrier, here, we ruled out the direct Pd(II)/Pd(IV) oxidation by AcOO^tBu, and hypothesized that the reaction with AcOO^tBu may undergo via a different mechanism, which may involve the ligand exchange with solvent (HFIP) or with the in-situ generate byproduct (H₂O).

38. Kitaura, K.; Morokuma, K., A New Energy Decomposition Scheme for Molecular Interactions within the Hartree-Fock Approximation. *Int. J. Quantum Chem.* **1976**, *10*, 325-340.

39. Nagase, S.; Morokuma, K., An ab initio Molecular Orbital Study of Organic Reactions. The Energy, Charge, and Spin Decomposition Analyses at the Transition State and along the Reaction Pathway. *J. Am. Chem. Soc.* **1978**, *100*, 1666-1672.

40. Bickelhaupt, F. M., Understanding Reactivity with Kohn–Sham Molecular Orbital Theory: E2-S_N2 Mechanistic Spectrum and other Concepts. *J. Comput. Chem.* **1999**, *20*, 11-128

41. Diefenbach, A.; Bickelhaupt, F. M., Oxidative Addition of Pd to C–H, C–C and C–Cl Bonds: Importance of Relativistic Effects in DFT calculations. *J. Chem. Phys.* **2001**, *115*, 4030-4040.

42. Bickelhaupt, F. M.; Houk, K. N., Analyzing Reaction Rates with the Distortion/Interaction-Activation Strain Model. *Angew. Chem. Int. Ed.* **2017**, *56*, 10070-10086.

43. Ess, D. H.; Houk, K. N., Theory of 1,3-Dipolar Cycloadditions: Distortion/Interaction and Frontier Molecular Orbital Models. *J. Am. Chem. Soc.* **2008**, *130*, 10187-10198.

44. Green, A. G.; Liu, P.; Merlic, C. A.; Houk, K. N., Distortion/Interaction Analysis Reveals the Origins of Selectivities in Iridium-Catalyzed C–H Borylation of Substituted Arenes and 5-Membered Heterocycles. *J. Am. Chem. Soc.* **2014**, *136*, 4575-4583.

45. Liu, F.; Paton, R. S.; Kim, S.; Liang, Y.; Houk, K. N., Diels-Alder Reactivities of Strained and Unstrained Cycloalkenes with Normal and Inverse-Electron-Demand Dienes: Activation Barriers and Distortion/Interaction Analysis. *J. Am. Chem. Soc.* **2013**, *135*, 15642-15649.

46. As seen in Figure 6, the C–H bond of the substrate has been elongated more in **4s-ts** (1.46 Å) than in **4-ts** (1.38 Å). Furthermore, ideally, the dihedral angle of the C₃C₆C₉C₁₀ in the substrate should be near 180°, i.e., the terminal γ methyl group and the carboxylate group should be in a favored staggered conformation (Figure 6b). In **4-ts**, the dihedral angle is 173.51°, which is closer to the staggered conformation. However, in **4s-ts**, because of the close contact between the γ-methyl group and the ligand, it decreased to 165.46°.

47. Yang, Y.-F.; Chen, G.; Hong, X.; Yu, J.-Q.; Houk, K. N., The Origins of Dramatic Differences in Five-membered vs Six-membered Chelation of Pd(II) on Efficiency of C(sp³)-H Bond Activation. *J. Am. Chem. Soc.* **2017**, *139*, 8514-8521.

48. Jin X.; Xu, H.; Zhao, N.; Li R.; Dang, Y., Origins of Unconventional γ Site Selectivity in Palladium-catalyzed C(sp³)-H Activation and Arylation of Aliphatic Alcohols. *Org. Lett.* **2020**, *22*, 1464-1468.

49. Frisch, M. J.; Trucks, G. W.; Schlegel, H. B.; Scuseria, G. E.; Robb, M. A.; Cheeseman, J. R.; Scalmani, G.; Barone, V.; Petersson, G. A.; Nakatsuji, H.; Li, X.; Caricato, M.; Marenich, A. V.; Bloino, J.; Janesko, B. G.; Gomperts, R.; Mennucci, B.; Hratchian, H. P.; Ortiz, J. V.; Izmaylov, A. F.; Sonnenberg, J. L.; Williams-Young, D.; Ding, F.; Lipparini, F.; Egidi, F.; Goings, J.; Peng, B.; Petrone, A.; Henderson, T.; Ranasinghe, D.; Zakrzewski, V. G.; Gao, J.; Rega, N.; Zheng, G.; Liang, W.; Hada, M.; Ehara, M.; Toyota, K.; Fukuda, R.; Hasegawa, J.; Ishida, M.; Nakajima, T.; Honda, Y.; Kitao, O.; Nakai, H.; Vreven, T.; Throssell, K.; Montgomery, J. A., Jr.; Peralta, J. E.; Ogliaro, F.; Bearpark, M. J.; Heyd, J. J.; Brothers, E. N.; Kudin, K. N.; Staroverov, V. N.; Keith, T. A.; Kobayashi, R.; Normand, J.; Raghavachari, K.; Rendell, A. P.; Burant, J. C.; Iyengar, S. S.; Tomasi, J.; Cossi, M.; Millam, J. M.; Klene, M.; Adamo, C.; Cammi, R.; Ochterski, J. W.; Martin, R. L.; Morokuma, K.; Farkas, O.; Foresman, J. B.; Fox, D. J., *Gaussian 09, Revision D.01*, Gaussian, Inc., Wallingford CT, **2009**.

50. Becke, A. D., Density-functional Exchange-energy Approximation with Correct Asymptotic Behavior. *Phys. Rev. A* **1988**, *38*, 3098-3100.

51. Lee, C.; Yang, W.; Parr, R. G., Development of the Colle-Salvetti Correlation-energy Formula into a Functional of the Electron density. *Phys. Rev. B* **1988**, *37*, 785-789.

52. Becke, A. D., A New Mixing of Hartree – Fock and Local Density – Functional Theories. *J. Chem. Phys.* **1993**, *98*, 1372-1377.

53. Grimme, S.; Antony, J.; Ehrlich, S.; Krieg, H., A Consistent and Accurate ab initio Parametrization of Density Functional Dispersion Correction (DFT-D) for the 94 Elements H–Pu. *J. Chem. Phys.* **2010**, *132*, 154104.

54. Hay, P. J.; Wadt, W. R., Ab initio Effective Core Potentials for Molecular Calculations. Potentials for K to Au including the Outermost Core Orbitals. *J. Chem. Phys.* **1985**, *82*, 299-310.

55. Wadt, W. R.; Hay, P. J., Ab initio Effective Core Potentials for Molecular Calculations. Potentials for Main Group Elements Na to Bi. *J. Chem. Phys.* **1985**, *82*, 284-298.

56. Marenich, A. V.; Cramer, C. J.; Truhlar, D. G., Universal Solvation Model Based on Solute Electron Density and on a Continuum Model

of the Solvent Defined by the Bulk Dielectric Constant and Atomic Surface Tensions. *J. Phys. Chem. B* **2009**, *113*, 6378-6396.

57. CYLview, 1.0b; Legault, C. Y., Université de Sherbrooke, **2009** (<http://www.cylview.org>).

Table of Contents

